

Observer-Based Spatial Control of Advanced Heavy Water Reactor Using Time-Scale Decoupling

Ravindra Munje¹, Danying Gu, Ranvir Desai, Balasaheb Patre, and Weidong Zhang²

Abstract—The 90th-order system of advanced heavy water reactor (AHWR) exhibits a three-time-scale structure with 38 slow, 35 fast, and 17 fastest state variables. Consequently, an effective controller is needed to regulate the spatial power. If the controller is based on state feedback, its realization needs an accurate and precise state observer. The regular design of a full or even reduced-order observer for such a three-time-scale system is a challenging task which, however, can be addressed by time-scale decoupling. In this paper, full- and reduced-order observers are proposed for the singularly perturbed three-time-scale system by a novel method. The novelty lies in the fact that the presented multistage observer designs help to reduce design complexity and computational time without losing the freedom to design independent observer gains for slow, fast, and fastest subsystems. These observers are then employed for the state estimation of AHWR, which are fed to the feedback controller for spatial stabilization. Performances of these observers, evaluated on the nonlinear model of AHWR in the presence of transients, are compared with the controller without an observer and fast output sampling-based controller. It is seen that the estimated values are in close agreement with the actual values due to which the controller performance is found to be satisfactory with the observers.

Index Terms—Advanced heavy water reactor (AHWR), state estimation, state observer, three-time-scale system, two-time-scale system.

NOMENCLATURE

Notation: Variables and parameters used in advanced heavy water reactor (AHWR) model.

C	Delayed neutron precursor concentration.
E_e	Average thermal energy liberated per fission, J.

Manuscript received July 16, 2018; revised September 10, 2018; accepted September 24, 2018. Date of publication October 4, 2018; date of current version November 14, 2018. This work was supported in part by the National Science Foundation of China under Grant 61750110524, Grant 61473183, Grant U1509211, and Grant 61627810 and in part by the National Key Research and Development Program of China under Grant SQ2017YFGH001005. (Corresponding author : Weidong Zhang.)

R. Munje is with the Department of Automation, Shanghai Jiao Tong University, Shanghai 200240, China, and also with the K. K. Wagh Institute of Engineering Education and Research, Nashik 422003, India (e-mail: ravimunjje@yahoo.co.in).

D. Gu is with the Shanghai Nuclear Engineering Research and Design Institute, Shanghai 200233, China (e-mail: gudanying@snerdi.com.cn).

R. Desai and B. Patre are with the Shri Guru Gobind Singhji Institute of Engineering and Technology, Nanded 431606, India (e-mail: ranvirdesai@nanded@gmail.com; bmpatre@ieee.org).

W. Zhang is with the Department of Automation, Shanghai Jiao Tong University, Shanghai 200240, China (e-mail: wdzhang@sjtu.edu.cn).

Color versions of one or more of the figures in this paper are available online at <http://ieeexplore.ieee.org>.

Digital Object Identifier 10.1109/TNS.2018.2873803

H	Position of regulating rod (RR), % in.
I	Iodine concentration.
P	Fission power, MW.
V	Volume, m ³ .
X	Xenon concentration.
e_{vx}, e_x	Constants of thermal hydraulics model.
h	Enthalpy, kJ/kg.
q	Mass flow rate, kg/s.
v	Voltage signal to RR drive, V.
x	Exit mass quality.
α	Coupling coefficient.
β	Delayed neutron fraction.
γ	Fraction fission yield.
λ	Decay constant.
ℓ	The prompt neutron life time, s.
ρ	Reactivity, k.
σ_a	Microscopic absorption cross section, cm ² .
Σ_f	Macroscopic fission cross section, cm ⁻¹ .
κ	Constant of RR position.
δ	Deviation parameter.

Notation: Subscripts used in AHWR model.

C	Precursor.
H	Position of RR.
I	Iodine.
P	Power.
X	Xenon.
c	Vaporization.
d	Downcomer.
f	Feed water.
i, j	Node number.
k	RR number.
s	Steam.
t	Total power.
w	Water.
x	Exit mass quality.

I. INTRODUCTION

THE nuclear energy is accepted worldwide as an economically viable, environmentally friendly, and implementable option on a large scale in order to minimize the greenhouse gas emissions in near future produced by fossil fuel consumption. As a result, the world's nuclear energy generation is expected to increase to 554 GWe by 2030 and to 874 GWe by 2050 in the high case [1]. This raises the issues of safety and stability of nuclear power plants. In this regards, an exact knowledge of the immeasurable variables is essential in a nuclear reactor

to devise an impressive power control. The estimation of states of the nuclear power plant has been investigated for a long time [2]. In [3], neutron flux, xenon, and iodine concentrations are estimated by a Luenberger-type observer from the output measurements. Since the nuclear reactor dynamics are a function of fuel burnup, spatial power distribution, productions of xenon, and delayed neutrons, the robust observer is mandatory for the state estimation. Therefore, the robust sliding mode observers (SMOs) are submitted in [4] and [5]. Nevertheless, the SMO is accompanied by the undesirable chattering, resulting in the performance degradation of the system. Hence, higher order SMOs (HOSMOs) are suggested for observation of precursors' concentrations [6], reactivity and fuel temperature [7], and xenon and samarium concentrations [8]. Although the HOSMOs provide closeness between the actual and computed states, they are less suitable for the real-time implementation due to the large control input and tracking errors.

As the reactivity depends on many factors, it is very painful to model it mathematically. Therefore, it is modeled as an extended state variable to calculate the neutron flux and precursor concentrations [9]. Furthermore, a wavelet-based multiscale extended Kalman filtering technique is reported in [10]. All the estimation algorithms recommended earlier are tested on a point kinetic model (PKM) of a nuclear reactor, with a varied number of delayed neutron groups. Nonetheless, PKM is not valid in case of large reactors as the flux shape experiences substantial variation with respect to time. For that reason, 56th-order model of pressurized heavy water reactor is developed, for exclusive consideration of the flux shape variation, and a reduced-order linear observer is examined [11]. It is worth mentioning here that the large nuclear reactors belong to the special class of systems called singularly perturbed systems. The straightforward design of a full or even reduced-order observer for such systems can have ill-conditioning problems. In this situation, the observer designed by time-scale separation is the best choice, in which the original system is decoupled into lower order subsystems having well-conditioned matrices [12]. Thereof, independent designs can be accomplished for the subsystem observers, and the results can be combined to yield a composite observer gain for the primary system. Full- and reduced-order observer designs [13], [14] for the singularly perturbed two-time-scale system formulated by quasi-steady-state modeling involves approximation. More recently, H. Yoo *et al.* [15], [16] have come up with new designs for full- and reduced-order observers with high accuracy using direct block diagonalization of the singularly perturbed two-time-scale system.

The stochastic estimators [10] are built using a probability distribution function, making them highly reliable and versatile for quick estimation of states. Conversely, the computational complexity involved in using them makes them unrealistic for singularly perturbed multitime-scale systems, such as two-time-scale and three-time-scale systems. Further to add, the numerical stiffness of the three-time-scale system is much greater than the two-time-scale system due to the occurrence of multiple eigenvalue clusters of widely different speeds. Furthermore, the nonlinear observers [6]–[8],

even though work excellently for the nonlinear plants, their practical applicability has a limitation too. On the contrary, application of the linear observers is well appreciated due to their significant roles in both theory and practice [17], [18]. In this paper, motivated by [15] and [16], linear observers are proposed for the singularly perturbed three-time-scale system. The undertaken work is also provoked by the fact that besides a variety of feedback control proposals for advanced heavy water reactor (AHWR) [19], there is a little work on the spatial control of AHWR via observers.

This paper suggests full- and reduced-order observers for the singularly perturbed three-time-scale system separately by three-stage and two-stage designs. Full-order observer computes all the states, whereas the reduced-order observer computes selective states. The three-stage design is carried out using the two-time-scale similarity transformations, in contrast to the three-time-scale transformation used in [20]. Also, both two-stage and three-stage designs are accomplished by solving less number of algebraic questions compared to [15] and [20], respectively. As a deduction, the design complexity and computation time are significantly diminished. Observers obtained using the outlined procedure are then integrated with the feedback controller, designed in [21], and the performance of the nonlinear model of the AHWR is analyzed under transients by comparing results with the controller without an observer as well as the fast output sampling-based controller. Rest of the paper is structured as follows. A brief description of the AHWR plant is given in Section II. In Section III, full- and reduced-order observer schemes for a three-time-scale system are proposed. Section IV reveals the applicability of these observers to an explicit singularly perturbed model of AHWR. Simulations of a nonlinear AHWR model with observer and controller are described in Section V, followed by the conclusion in Section VI.

II. AHWR PLANT DESCRIPTION

For mathematical modeling, the reactor core of AHWR is divided into 17 relatively large fictitious nodes. The complete model is delineated by the following nonlinear equations [22]:

$$\frac{dP_i}{dt} = (\rho_i - a_{ii} - \beta) \frac{P_i}{\ell} + \sum_{j=1}^{17} a_{ji} \frac{P_j}{\ell} + \lambda C_i \quad (1)$$

$$\frac{dC_i}{dt} = \frac{\beta}{\ell} P_i - \lambda C_i \quad (2)$$

$$\frac{dI_i}{dt} = \gamma_I \sum_{f,i} P_i - \lambda_I I_i \quad (3)$$

$$\frac{dX_i}{dt} = \gamma_X \sum_{f,i} P_i + \lambda_I I_i - (\lambda_X + \bar{\sigma}_{Xi} P_i) X_i \quad (4)$$

$$\frac{dH_k}{dt} = \kappa v_k \quad (5)$$

$$e_{vxi} \frac{dx_i}{dt} = P_i - q_{di}(h_w - h_d) - q_{di} x_i h_c \quad (6)$$

$$e_{xi} \frac{dh_d}{dt} = q_f(\hat{k}_2 h_f - \hat{k}_1) - q_d(\hat{k}_2 h_d - \hat{k}_1) \quad (7)$$

where $i = 1, 2, \dots, 17$ and $k = 2, 4, 6, 8$. P , C , I , X , H , x , and h_d are, respectively, the nodal powers, single-group delayed neutron precursor, iodine, and xenon concentrations,

regulating rod (RR) positions, exit quality, and downcomer enthalpy. $\bar{\sigma}_{Xi} = \sigma_{Xi}/E_e \Sigma_{fi} V_i$, $\hat{k}_2 = h_s/h_c$, and $\hat{k}_1 = h_w \hat{k}_2$. v_k is the control signal applied to the RR drive. All the variables and parameters along with subscripts used in this model are defined in the Nomenclature. Values of e_{vXi} , e_{Xi} , and other constants are specified in [22]. The overall reactivity is designated by ρ_i in (1) and is expressed as $\rho_i = \rho_{iu} + \rho_{iX} + \rho_{ix}$, where ρ_{iu} , ρ_{iX} , and ρ_{ix} are the reactivity feedbacks due to the control rods, xenon, and coolant void fraction, respectively. Linearizing (1)–(7) around the steady state, a standard state-space representation can be acquired by defining a state vector

$$\mathbf{x} = [\mathbf{x}_H^T \ \mathbf{x}_X^T \ \mathbf{x}_I^T \ \delta h_d \ \mathbf{x}_C^T \ \mathbf{x}_x^T \ \mathbf{x}_P^T]^T \quad (8)$$

where $\mathbf{x}_H = [\delta H_2 \ \delta H_4 \ \delta H_6 \ \delta H_8]^T$ and the rest $\mathbf{x}_\xi = [(\delta \xi_1/\xi_{10}) \ \cdots \ (\delta \xi_{17}/\xi_{170})]^T$, $\xi = X, I, C, x, P$, in which δ stands for the deviation from respective steady-state value. Similarly, input and output vectors are expounded as

$$\mathbf{u} = [\delta v_2 \ \delta v_4 \ \delta v_6 \ \delta v_8]^T \quad (9)$$

$$\mathbf{y} = [y_t \ y_1 \ \cdots \ y_{17}]^T \quad (10)$$

where $y_t = \sum_{i=1}^{17} (\delta P_i / (\sum_{j=1}^{17} P_{j0}))$ and $y_i = (\delta P_i / P_{i0})$ are, respectively, the normalized total reactor power and nodal powers, in which P_{i0} is a steady-state value of nodal power. Eventually, the system (1)–(7) is expressed as

$$\dot{\mathbf{x}} = \hat{\mathbf{A}}\mathbf{x} + \mathbf{B}\mathbf{u} + \mathbf{B}_f \delta q_f \quad (11)$$

$$\mathbf{y} = \mathbf{C}\mathbf{x} \quad (12)$$

where q_f is the flow rate of feed water. This system is ascertained to be controllable and observable. The eigenvalues of system matrix $\hat{\mathbf{A}}$ are noticed to be falling into three broadly separated clusters. The first cluster has 38 “slow” eigenvalues ranging from -1.8870×10^{-4} to 7.455×10^{-3} . Second cluster is having 35 “fast” eigenvalues ranging from -1.2514×10^{-2} to -1.8395×10^{-1} , and the third cluster contains 17 “fastest” eigenvalues ranging from -7.2516 to -2.7626×10^2 . It is confirmed that all the eigenvalues in the fast and fastest clusters are in the left half of s plane while the slow cluster includes six eigenvalues in the right half and four at the origin. This indicates instability, demanding a competent spatial power feedback controller for stable and steady operation of AHWR. Normally, the control of large nuclear reactors comprises control of total as well as spatial power, that is,

$$\mathbf{u} = \mathbf{u}_t + \mathbf{u}_s \quad (13)$$

where \mathbf{u}_t and \mathbf{u}_s are, respectively, the total and spatial power feedback components. Thus, before designing any spatial power controller, total power control is established. The total power control of AHWR is achieved by generating control signals for RRs, based on the total power feedback as

$$\mathbf{u}_t = -\mathbf{K}\mathbf{y} \quad (14)$$

where (4×18) order matrix $\mathbf{K} = [\mathbf{k}_t \ \mathbf{0} \ \cdots \ \mathbf{0}]$. Here, $\mathbf{0}$ is a column vector of order 4 and $\mathbf{k}_t = [k_t \ k_t \ k_t \ k_t]^T$, such that the feedback gain corresponding to total power is k_t for all RRs

and is zero corresponding to nodal powers. Using (12)–(14), the state equation (11) changes to

$$\dot{\mathbf{x}} = \mathbf{A}\mathbf{x} + \mathbf{B}\mathbf{u}_s + \mathbf{B}_f \delta q_f \quad (15)$$

where $\mathbf{A} = (\hat{\mathbf{A}} - \mathbf{B}\mathbf{K})$. The total power control is succeeded by setting $k_t = 12.5$ [22]. Even after the total power feedback, the system $(\mathbf{A}, \mathbf{B}, \mathbf{C})$ is observed to be controllable and observable. Besides, the system matrix \mathbf{A} is also witnessed to possess three groups of eigenvalues of the same orders as that of $\hat{\mathbf{A}}$ with no change in the locations of eigenvalues in the fast and fastest groups. On the other hand, in a slow cluster still four eigenvalues with positive real parts and three eigenvalues at the origin are noticed. In view of that, even if the total power in the reactor is maintained steady with input (14), the power in the various regions of the reactor core may undergo oscillations and that being so, spatial-feedback control is essential.

In case of AHWR, the neutron flux is determined using out-of-core ion chambers and in-core detectors. The total power of the reactor is inferred from ion chambers in low-power range and in-core detectors [23]. The application of state feedback-based spatial power controller for AHWR involves two main concerns, namely, acquiring estimates of immeasurable states by an observer and designing an observer for the higher order system. In other words, as some of the state variables like xenon, iodine, and precursors' concentrations cannot be measured by sensors, an observer is desired to determine them exactly. Contrarily, designing an observer for a high-dimensional system, having state variables moving at distinctly different speeds, would be computationally challenging. This difficulty is overcome by the observers claimed in this paper.

III. OBSERVERS FOR THREE-TIME-SCALE SYSTEM

Consider a linear time-invariant three-time-scale system consisting of $\mathbf{x}_1 \in \mathfrak{R}^{n_1}$ slow, $\mathbf{x}_2 \in \mathfrak{R}^{n_2}$ fast, and $\mathbf{x}_3 \in \mathfrak{R}^{n_3}$ fastest states as

$$\left. \begin{aligned} \dot{\mathbf{x}}_1 &= \mathbf{A}_{11}\mathbf{x}_1 + \mathbf{A}_{12}\mathbf{x}_2 + \mathbf{A}_{13}\mathbf{x}_3 + \mathbf{B}_1\mathbf{u} \\ \mu\dot{\mathbf{x}}_2 &= \mathbf{A}_{21}\mathbf{x}_1 + \mathbf{A}_{22}\mathbf{x}_2 + \mathbf{A}_{23}\mathbf{x}_3 + \mathbf{B}_2\mathbf{u} \\ \epsilon\dot{\mathbf{x}}_3 &= \mathbf{A}_{31}\mathbf{x}_1 + \mathbf{A}_{32}\mathbf{x}_2 + \mathbf{A}_{33}\mathbf{x}_3 + \mathbf{B}_3\mathbf{u} \\ \mathbf{y} &= \mathbf{C}_1\mathbf{x}_1 + \mathbf{C}_2\mathbf{x}_2 + \mathbf{C}_3\mathbf{x}_3 \end{aligned} \right\} \quad (16)$$

with $n_1 + n_2 + n_3 = n$. $\mathbf{u} \in \mathfrak{R}^m$, $\mathbf{y} \in \mathfrak{R}^p$, and let $\mathbf{x} = [\mathbf{x}_1^T \ \mathbf{x}_2^T \ \mathbf{x}_3^T]^T$

$$\mathbf{A} = \begin{bmatrix} \mathbf{A}_{11} & \mathbf{A}_{12} & \mathbf{A}_{13} \\ \frac{\mathbf{A}_{21}}{\mu} & \frac{\mathbf{A}_{22}}{\mu} & \frac{\mathbf{A}_{23}}{\mu} \\ \frac{\mathbf{A}_{31}}{\epsilon} & \frac{\mathbf{A}_{32}}{\epsilon} & \frac{\mathbf{A}_{33}}{\epsilon} \end{bmatrix}, \quad \mathbf{B} = \begin{bmatrix} \mathbf{B}_1 \\ \frac{\mathbf{B}_2}{\mu} \\ \frac{\mathbf{B}_3}{\epsilon} \end{bmatrix}, \quad \mathbf{C}^T = \begin{bmatrix} \mathbf{C}_1^T \\ \mathbf{C}_2^T \\ \mathbf{C}_3^T \end{bmatrix}.$$

Matrices \mathbf{A}_{ij} , \mathbf{B}_i , and \mathbf{C}_i are of proper orders. μ and ϵ specify speed ratios of \mathbf{x}_1 versus \mathbf{x}_2 and \mathbf{x}_1 versus \mathbf{x}_3 states, respectively, such that $\epsilon \ll \mu \ll 1$. More specifically, the system (16) has three distinct clusters of eigenvalues in which n_1 eigenvalues are near the origin, and n_2 and n_3 eigenvalues are far and farther from the origin. If the eigenvalues of \mathbf{A} are arranged in the increasing order of their magnitudes as

$$\psi(\mathbf{A}) = (\psi_1, \dots, \psi_{n_1}, \psi_{n_1+1}, \dots, \psi_{n_1+n_2}, \psi_{n_1+n_2+1}, \dots, \psi_n)$$

where ψ_i is i th eigenvalue with

$$0 \leq |\psi_1| < \dots < |\psi_{n_1}| \ll |\psi_{n_1+1}| \\ < \dots < |\psi_{n_1+n_2}| \ll |\psi_{n_1+n_2+1}| < \dots < |\psi_n|$$

then referring [24]

$$\mu = \frac{|\psi_{n_1}|}{|\psi_{n_1+1}|} \quad \text{and} \quad \epsilon = \frac{|\psi_{n_1}|}{|\psi_{n_1+n_2+1}|}.$$

Before proceeding further, the following assumptions are imposed on (16).

Assumption 1: The pair (\mathbf{A}, \mathbf{B}) is controllable and pair (\mathbf{A}, \mathbf{C}) is observable.

Assumption 2: Matrix \mathbf{C} of every redefined system, contemplated for reduced-order observer design has a full rank, i.e., equal to the number of outputs available for measurement.

Assumption 3: Matrices \mathbf{A}_{33} and \mathbf{A}_{22} are invertible [24].

Assumptions 1 and 2 are enforced to calculate observer gains and to satisfy the observability condition of the reduced-order subsystems. Assumption 3 is a standard assumption in the time-scale theory and is useful to get the solutions of algebraic equations. In what follows, full- and reduced-order observers, suggested for the system (16) are presented.

A. Full-Order Observer Design

The computational difficulty in deriving an observer gain for a numerically ill-conditioned system (16) is efficiently lessened by the three-stage design, elaborated by duality principle. Since transpose of the observer feedback matrix, i.e., $(\mathbf{A}^T - \mathbf{C}^T \mathbf{L}^T)$ generates the dual form to the system feedback matrix $(\mathbf{A} - \mathbf{B}\mathbf{K})$, similar approach can be adapted to design feedback matrices for $\dot{\mathbf{x}} = (\mathbf{A} - \mathbf{B}\mathbf{K})\mathbf{x}$ and $\dot{\hat{\mathbf{x}}} = (\mathbf{A} - \mathbf{L}\mathbf{C})\hat{\mathbf{x}} + \mathbf{L}\mathbf{y}$, and therefore, think of an analogous system to (16) as

$$\begin{bmatrix} \dot{\mathbf{z}}_1 \\ \dot{\mathbf{z}}_2 \\ \dot{\mathbf{z}}_3 \end{bmatrix} = \begin{bmatrix} \mathbf{A}_{11}^T & \frac{\mathbf{A}_{21}^T}{\mu} & \frac{\mathbf{A}_{31}^T}{\epsilon} \\ \mathbf{A}_{12}^T & \frac{\mathbf{A}_{22}^T}{\mu} & \frac{\mathbf{A}_{32}^T}{\epsilon} \\ \mathbf{A}_{13}^T & \frac{\mathbf{A}_{23}^T}{\mu} & \frac{\mathbf{A}_{33}^T}{\epsilon} \end{bmatrix} \begin{bmatrix} \mathbf{z}_1 \\ \mathbf{z}_2 \\ \mathbf{z}_3 \end{bmatrix} + \begin{bmatrix} \mathbf{C}_1^T \\ \mathbf{C}_2^T \\ \mathbf{C}_3^T \end{bmatrix} \mathbf{v}. \quad (17)$$

Introducing

$$\begin{bmatrix} \mathbf{q}_1 \\ \mathbf{q}_2 \\ \mathbf{q}_3 \end{bmatrix} = \begin{bmatrix} \mathbf{I}_{n_1} & \mathbf{0} & \mathbf{0} \\ \mathbf{0} & \frac{\mathbf{I}_{n_2}}{\mu} & \mathbf{0} \\ \mathbf{0} & \mathbf{0} & \frac{\mathbf{I}_{n_3}}{\epsilon} \end{bmatrix} \begin{bmatrix} \mathbf{z}_1 \\ \mathbf{z}_2 \\ \mathbf{z}_3 \end{bmatrix} = \mathbf{T} \begin{bmatrix} \mathbf{z}_1 \\ \mathbf{z}_2 \\ \mathbf{z}_3 \end{bmatrix} \quad (18)$$

system (17) is transformed into an explicitly singularly perturbed form

$$\begin{bmatrix} \dot{\mathbf{q}}_1 \\ \dot{\mathbf{q}}_2 \\ \dot{\mathbf{q}}_3 \end{bmatrix} = \begin{bmatrix} \mathbf{A}_{11}^T & \mathbf{A}_{21}^T & \mathbf{A}_{31}^T \\ \frac{\mathbf{A}_{12}^T}{\mu} & \frac{\mathbf{A}_{22}^T}{\mu} & \frac{\mathbf{A}_{32}^T}{\mu} \\ \frac{\mathbf{A}_{13}^T}{\epsilon} & \frac{\mathbf{A}_{23}^T}{\epsilon} & \frac{\mathbf{A}_{33}^T}{\epsilon} \end{bmatrix} \begin{bmatrix} \mathbf{q}_1 \\ \mathbf{q}_2 \\ \mathbf{q}_3 \end{bmatrix} + \begin{bmatrix} \mathbf{C}_1^T \\ \mathbf{C}_2^T \\ \mathbf{C}_3^T \end{bmatrix} \mathbf{v} \quad (19)$$

where \mathbf{I}_n is an identity matrix of order n , $\mathbf{q}_1 \in \mathbb{R}^{n_1}$, $\mathbf{q}_2 \in \mathbb{R}^{n_2}$, and $\mathbf{q}_3 \in \mathbb{R}^{n_3}$. For designing an observer in three stages,

first of all, the system (19) is changed to lower triangular form and then observer gains are designed independently for slow, fast, and fastest subsystems by two-time-scale similarity transformations. Now, regrouping states of (19) as $\mathbf{q}_a = [\mathbf{q}_1^T \ \mathbf{q}_2^T]^T$ and $\mathbf{q}_b = \mathbf{q}_3$ result in

$$\begin{bmatrix} \dot{\mathbf{q}}_a \\ \dot{\mathbf{q}}_b \end{bmatrix} = \begin{bmatrix} \frac{\bar{\mathbf{A}}_{11}^T}{\epsilon} & \frac{\bar{\mathbf{A}}_{21}^T}{\epsilon} \\ \frac{\bar{\mathbf{A}}_{12}^T}{\epsilon} & \frac{\bar{\mathbf{A}}_{22}^T}{\epsilon} \end{bmatrix} \begin{bmatrix} \mathbf{q}_a \\ \mathbf{q}_b \end{bmatrix} + \begin{bmatrix} \bar{\mathbf{C}}_1^T \\ \bar{\mathbf{C}}_2^T \end{bmatrix} \mathbf{v} \quad (20)$$

where $\bar{\mathbf{A}}_{ij}$ and $\bar{\mathbf{C}}_i$ are updated accordingly. The system (20) is the two-time-scale representation of (19), where n_1 “slow” and n_2 “fast” states are merged to form $(n_1 + n_2)$ “slow” states and n_3 “fastest” states are taken as “fast” states. Now, applying

$$\mathbf{q}_s = \mathbf{q}_a + \epsilon \mathbf{P}^T \mathbf{q}_b \quad (21)$$

to the system (20), produces

$$\begin{bmatrix} \dot{\mathbf{q}}_s \\ \dot{\mathbf{q}}_b \end{bmatrix} = \begin{bmatrix} \frac{\bar{\mathbf{A}}_s^T}{\epsilon} & \mathbf{0} \\ \frac{\bar{\mathbf{A}}_f^T}{\epsilon} & \frac{\bar{\mathbf{A}}_f^T}{\epsilon} \end{bmatrix} \begin{bmatrix} \mathbf{q}_s \\ \mathbf{q}_b \end{bmatrix} + \begin{bmatrix} \bar{\mathbf{C}}_s^T \\ \bar{\mathbf{C}}_f^T \end{bmatrix} \mathbf{v} \quad (22)$$

where $\bar{\mathbf{A}}_s^T = \bar{\mathbf{A}}_{11}^T + \mathbf{P}^T \bar{\mathbf{A}}_{12}^T$, $\bar{\mathbf{A}}_f^T = \bar{\mathbf{A}}_{22}^T - \epsilon \bar{\mathbf{A}}_{12}^T \mathbf{P}^T$, $\bar{\mathbf{C}}_s = \bar{\mathbf{C}}_1^T + \mathbf{P}^T \bar{\mathbf{C}}_2^T$ and

$$\bar{\mathbf{A}}_{21}^T + \mathbf{P}^T \bar{\mathbf{A}}_{22}^T - \epsilon (\bar{\mathbf{A}}_{11}^T + \mathbf{P}^T \bar{\mathbf{A}}_{12}^T) \mathbf{P}^T = 0. \quad (23)$$

The unique solution of \mathbf{P}^T is gained by solving (23) by fixed point iteration method, using the first-order approximation as $\mathbf{P}^{T(0)} = -\bar{\mathbf{A}}_{21}^T (\bar{\mathbf{A}}_{22}^T)^{-1}$, for sufficiently small value of ϵ under the Assumption 3 [24]. Accordingly, (22) is modified to lower triangular form, where \mathbf{q}_s is completely decoupled from \mathbf{q}_b . Recall that, \mathbf{q}_s combines n_1 “slow” and n_2 “fast” states of the system (19). Due to this, (22) can also be written in two-time-scale form, by partitioning matrices $\bar{\mathbf{A}}_s^T$ and $\bar{\mathbf{C}}_s^T$ suitably, as

$$\begin{bmatrix} \dot{\mathbf{q}}_{s1} \\ \dot{\mathbf{q}}_{s2} \end{bmatrix} = \begin{bmatrix} \frac{\bar{\mathbf{A}}_{s11}^T}{\mu} & \frac{\bar{\mathbf{A}}_{s21}^T}{\mu} \\ \frac{\bar{\mathbf{A}}_{s12}^T}{\mu} & \frac{\bar{\mathbf{A}}_{s22}^T}{\mu} \end{bmatrix} \begin{bmatrix} \mathbf{q}_{s1} \\ \mathbf{q}_{s2} \end{bmatrix} + \begin{bmatrix} \bar{\mathbf{C}}_{s1}^T \\ \bar{\mathbf{C}}_{s2}^T \end{bmatrix} \mathbf{v} \quad (24)$$

where $\mathbf{q}_s = [\mathbf{q}_{s1}^T \ \mathbf{q}_{s2}^T]^T$ with $\mathbf{q}_{s1} \in \mathbb{R}^{n_1}$ and $\mathbf{q}_{s2} \in \mathbb{R}^{n_2}$. At this moment, a linear transformation

$$\mathbf{q}_{ss} = \mathbf{q}_{s1} + \mu \mathbf{P}_s^T \mathbf{q}_{s2} \quad (25)$$

is applied to (24). Here, matrix \mathbf{P}_s^T is reckoned by solving

$$\bar{\mathbf{A}}_{s21}^T + \mathbf{P}_s^T \bar{\mathbf{A}}_{s22}^T - \mu (\bar{\mathbf{A}}_{s11}^T + \mathbf{P}_s^T \bar{\mathbf{A}}_{s12}^T) \mathbf{P}_s^T = 0. \quad (26)$$

Solution of \mathbf{P}_s^T can be obtained under Assumption 3 for a small value of μ in the same way as that of \mathbf{P}^T in (23). Resultantly, a lower triangular form of (24) is reached

$$\begin{bmatrix} \dot{\mathbf{q}}_{ss} \\ \dot{\mathbf{q}}_{s2} \end{bmatrix} = \begin{bmatrix} \frac{\bar{\mathbf{A}}_{ss}^T}{\mu} & \mathbf{0} \\ \frac{\bar{\mathbf{A}}_{sf}^T}{\mu} & \frac{\bar{\mathbf{A}}_{sf}^T}{\mu} \end{bmatrix} \begin{bmatrix} \mathbf{q}_{ss} \\ \mathbf{q}_{s2} \end{bmatrix} + \begin{bmatrix} \bar{\mathbf{C}}_{ss}^T \\ \bar{\mathbf{C}}_{s2}^T \end{bmatrix} \mathbf{v} \quad (27)$$

where $\bar{\mathbf{A}}_{ss}^T = \bar{\mathbf{A}}_{s11}^T + \mathbf{P}_s^T \bar{\mathbf{A}}_{s12}^T$, $\bar{\mathbf{A}}_{sf}^T = \bar{\mathbf{A}}_{s22}^T - \mu \bar{\mathbf{A}}_{s12}^T \mathbf{P}_s^T$, and $\bar{\mathbf{C}}_{ss}^T = \bar{\mathbf{C}}_{s1}^T + \mathbf{P}_s^T \bar{\mathbf{C}}_{s2}^T$. In such a way, using block triangular

forms (22) and (27) of two-time-scale systems, the original system (19) is converted into block triangular form

$$\begin{bmatrix} \dot{\mathbf{q}}_{ss} \\ \dot{\mathbf{q}}_{s2} \\ \dot{\mathbf{q}}_3 \end{bmatrix} = \begin{bmatrix} \bar{\mathbf{A}}_{ss}^T & \mathbf{0} & \mathbf{0} \\ \bar{\mathbf{A}}_{s12}^T & \bar{\mathbf{A}}_{sf}^T & \mathbf{0} \\ \frac{\mu}{\epsilon} \bar{\mathbf{A}}_{13}^T & \frac{\mu}{\epsilon} \bar{\mathbf{A}}_{23}^T & \bar{\mathbf{A}}_f^T \end{bmatrix} \begin{bmatrix} \mathbf{q}_{ss} \\ \mathbf{q}_{s2} \\ \mathbf{q}_3 \end{bmatrix} + \begin{bmatrix} \bar{\mathbf{C}}_{ss}^T \\ \bar{\mathbf{C}}_{s2}^T \\ \frac{\mu}{\epsilon} \bar{\mathbf{C}}_2^T \end{bmatrix} \nu \quad (28)$$

where $\bar{\mathbf{A}}_{12}^T$ is appropriately partitioned as $[\bar{\mathbf{A}}_{13}^T \quad \bar{\mathbf{A}}_{23}^T]$. The form (28) also satisfies the eigenvalue clustering property of three-time-scale system discussed earlier, i.e., subsystems $\bar{\mathbf{A}}_{ss}^T$, $((\bar{\mathbf{A}}_{sf}^T)/\mu)$, and $((\bar{\mathbf{A}}_f^T)/\epsilon)$ include, respectively, n_1 slow, n_2 fast, and n_3 fastest eigenvalues, such that

$$\max |\psi(\bar{\mathbf{A}}_{ss}^T)| \ll \min \left| \psi \left(\frac{\bar{\mathbf{A}}_{sf}^T}{\mu} \right) \right|$$

$$\max \left| \psi \left(\frac{\bar{\mathbf{A}}_{sf}^T}{\mu} \right) \right| \ll \min \left| \psi \left(\frac{\bar{\mathbf{A}}_f^T}{\epsilon} \right) \right|.$$

Now, one can proceed for three-stage observer gain design starting with \mathbf{q}_{ss} , i.e., the slow subsystem. To begin with, the input is designed for the system (27) and then for (22). In the first stage, applying

$$\nu = -\mathbf{L}_{ss}^T \mathbf{q}_{ss} + \nu_{sf} \quad (29)$$

to the system (27) leads to

$$\begin{bmatrix} \dot{\mathbf{q}}_{ss} \\ \dot{\mathbf{q}}_{s2} \end{bmatrix} = \begin{bmatrix} \bar{\mathbf{A}}_{ss}^T - \bar{\mathbf{C}}_{ss}^T \mathbf{L}_{ss}^T & \mathbf{0} \\ \frac{\bar{\mathbf{A}}_{s12}^T - \bar{\mathbf{C}}_{s2}^T \mathbf{L}_{ss}^T}{\mu} & \frac{\bar{\mathbf{A}}_{sf}^T}{\mu} \end{bmatrix} \begin{bmatrix} \mathbf{q}_{ss} \\ \mathbf{q}_{s2} \end{bmatrix} + \begin{bmatrix} \bar{\mathbf{C}}_{ss}^T \\ \frac{\bar{\mathbf{C}}_{s2}^T}{\mu} \end{bmatrix} \nu_{sf} \quad (30)$$

where \mathbf{L}_{ss}^T is selected, such that $\psi(\bar{\mathbf{A}}_{ss}^T - \bar{\mathbf{C}}_{ss}^T \mathbf{L}_{ss}^T) = \psi_s^{\text{desired}}$, where subscript “s” indicates slow subsystem. As the similarity transformations map the original system from one form to another without the loss of controllability (or observability), the pair $(\bar{\mathbf{A}}_{ss}^T, \bar{\mathbf{C}}_{ss}^T)$ is controllable [or the pair $(\bar{\mathbf{A}}_{ss}, \bar{\mathbf{C}}_{ss})$ is observable], due to which an arbitrary pole placement is possible under Assumption 1. Now, using

$$\mathbf{q}_{sf} = -\mathbf{M}_s^T \mathbf{q}_{ss} + \mathbf{q}_{s2} \quad (31)$$

system (30) is modified to

$$\begin{bmatrix} \dot{\mathbf{q}}_{ss} \\ \dot{\mathbf{q}}_{sf} \end{bmatrix} = \begin{bmatrix} \bar{\mathbf{A}}_{ss}^T - \bar{\mathbf{C}}_{ss}^T \mathbf{L}_{ss}^T & \mathbf{0} \\ \mathbf{0} & \frac{\bar{\mathbf{A}}_{sf}^T}{\mu} \end{bmatrix} \begin{bmatrix} \mathbf{q}_{ss} \\ \mathbf{q}_{sf} \end{bmatrix} + \begin{bmatrix} \bar{\mathbf{C}}_{ss}^T \\ \frac{\bar{\mathbf{C}}_{sf}^T}{\mu} \end{bmatrix} \nu_{sf} \quad (32)$$

where $\bar{\mathbf{C}}_{sf}^T = \bar{\mathbf{C}}_{s2}^T - \mu \mathbf{M}_s^T \bar{\mathbf{C}}_{ss}^T$ and

$$\bar{\mathbf{A}}_{s12}^T - \bar{\mathbf{C}}_{s2}^T \mathbf{L}_{ss}^T - \mu \mathbf{M}_s^T (\bar{\mathbf{A}}_{ss}^T - \bar{\mathbf{C}}_{ss}^T \mathbf{L}_{ss}^T) + \bar{\mathbf{A}}_{sf}^T \mathbf{M}_s^T = 0. \quad (33)$$

Matrix \mathbf{M}_s^T can be determined from (33) using fixed point iteration [with $\mathbf{M}_s^{(0)} = -(\bar{\mathbf{A}}_{sf}^T)^{-1}(\bar{\mathbf{A}}_{s12}^T - \bar{\mathbf{C}}_{s2}^T \mathbf{L}_{ss}^T)$ as the first-order approximation] and Assumption 4.

Assumption 4: $\psi(\bar{\mathbf{A}}_{ss}^T - \bar{\mathbf{C}}_{ss}^T \mathbf{L}_{ss}^T) \neq \psi((\bar{\mathbf{A}}_{sf}^T)/\mu)$.

Existence of $(\bar{\mathbf{A}}_{sf}^T)^{-1}$ is ensured by Assumption 3 and Assumption 4 is satisfied because $(\bar{\mathbf{A}}_{ss}^T - \bar{\mathbf{C}}_{ss}^T \mathbf{L}_{ss}^T)$ is designed to have desired “slow” eigenvalues, while $((\bar{\mathbf{A}}_{sf}^T)/\mu)$ has original

subsystem “fast” eigenvalues. In (32), subsystem \mathbf{q}_{sf} is made totally independent of \mathbf{q}_{ss} . Thereupon, in the second stage

$$\nu_{sf} = -\mathbf{L}_{sf}^T \mathbf{q}_{sf} \quad (34)$$

is passed to the system (32) as

$$\begin{bmatrix} \dot{\mathbf{q}}_{ss} \\ \dot{\mathbf{q}}_{sf} \end{bmatrix} = \begin{bmatrix} \bar{\mathbf{A}}_{ss}^T - \bar{\mathbf{C}}_{ss}^T \mathbf{L}_{ss}^T & \frac{-\bar{\mathbf{C}}_{ss}^T \mathbf{L}_{sf}^T}{\mu} \\ \mathbf{0} & \frac{\bar{\mathbf{A}}_{sf}^T - \bar{\mathbf{C}}_{sf}^T \mathbf{L}_{sf}^T}{\mu} \end{bmatrix} \begin{bmatrix} \mathbf{q}_{ss} \\ \mathbf{q}_{sf} \end{bmatrix} \quad (35)$$

so that $\psi((\bar{\mathbf{A}}_{sf}^T - \bar{\mathbf{C}}_{sf}^T \mathbf{L}_{sf}^T)/\mu) = \psi_f^{\text{desired}}$. The subscript “f” stands for fast subsystem. The controllability of $((\bar{\mathbf{A}}_{sf}^T)/\mu)$, $((\bar{\mathbf{C}}_{sf}^T)/\mu)$ is preserved due to Assumption 1. Thus, input for the system (24) is computed using (25), (29), (31), and (34) as

$$\nu = -\mathbf{L}_s^T [\mathbf{q}_{s1} \quad \mathbf{q}_{s2}]^T = -\mathbf{L}_s^T \mathbf{q}_s \quad (36)$$

where $\mathbf{L}_s^T = [\mathbf{L}_{ss}^T - \mathbf{L}_{sf}^T \mathbf{M}_s^T \quad \mu(\mathbf{L}_{ss}^T - \mathbf{L}_{sf}^T \mathbf{M}_s^T) \mathbf{P}_s^T + \mathbf{L}_{sf}^T]$. Actually, (36) is the input for \mathbf{q}_s , which is the decoupled part of (22). Therefore, the overall input ν has the form

$$\nu = -\mathbf{L}_s^T \mathbf{q}_s + \nu_f. \quad (37)$$

Passing on (37) to (22) and changing coordinates as

$$\mathbf{q}_f = -\mathbf{M}^T \mathbf{q}_s + \mathbf{q}_b \quad (38)$$

the subsystem \mathbf{q}_f is isolated from \mathbf{q}_s as

$$\begin{bmatrix} \dot{\mathbf{q}}_s \\ \dot{\mathbf{q}}_f \end{bmatrix} = \begin{bmatrix} \bar{\mathbf{A}}_s^T - \bar{\mathbf{C}}_s^T \mathbf{L}_s^T & \mathbf{0} \\ \mathbf{0} & \frac{\bar{\mathbf{A}}_f^T}{\epsilon} \end{bmatrix} \begin{bmatrix} \mathbf{q}_s \\ \mathbf{q}_f \end{bmatrix} + \begin{bmatrix} \bar{\mathbf{C}}_s^T \\ \frac{\bar{\mathbf{C}}_f^T}{\epsilon} \end{bmatrix} \nu_f \quad (39)$$

where $\bar{\mathbf{C}}_f^T = \bar{\mathbf{C}}_2^T - \epsilon \mathbf{M}^T \bar{\mathbf{C}}_s^T$ and \mathbf{M}^T is evaluated by setting

$$\bar{\mathbf{A}}_{12}^T - \bar{\mathbf{C}}_2^T \mathbf{L}_s^T - \epsilon \mathbf{M}^T (\bar{\mathbf{A}}_s^T - \bar{\mathbf{C}}_s^T \mathbf{L}_s^T) + \bar{\mathbf{A}}_f^T \mathbf{M}^T = 0 \quad (40)$$

similar to (33) with one more assumption.

Assumption 5: $\psi(\bar{\mathbf{A}}_s^T - \bar{\mathbf{C}}_s^T \mathbf{L}_s^T) \neq \psi(\bar{\mathbf{A}}_f^T/\epsilon)$.

It can be convinced by designing $(\bar{\mathbf{A}}_s^T - \bar{\mathbf{C}}_s^T \mathbf{L}_s^T)$ with desired eigenvalues laying in “slow” and “fast” modes. And, $(\bar{\mathbf{A}}_f^T/\epsilon)$ has “fastest” eigenvalues of (16). Finally, in the third stage

$$\nu_f = -\mathbf{L}_f^T \mathbf{q}_f \quad (41)$$

is applied to the system (39) as

$$\begin{bmatrix} \dot{\mathbf{q}}_s \\ \dot{\mathbf{q}}_f \end{bmatrix} = \begin{bmatrix} \bar{\mathbf{A}}_s^T - \bar{\mathbf{C}}_s^T \mathbf{L}_s^T & \frac{-\bar{\mathbf{C}}_s^T \mathbf{L}_f^T}{\epsilon} \\ \mathbf{0} & \frac{\bar{\mathbf{A}}_f^T - \bar{\mathbf{C}}_f^T \mathbf{L}_f^T}{\epsilon} \end{bmatrix} \begin{bmatrix} \mathbf{q}_s \\ \mathbf{q}_f \end{bmatrix} \quad (42)$$

so as to assign $\psi((\bar{\mathbf{A}}_f^T - \bar{\mathbf{C}}_f^T \mathbf{L}_f^T)/\epsilon) = \psi_{ff}^{\text{desired}}$, assuming the controllability of $((\bar{\mathbf{A}}_f^T)/\epsilon)$, $((\bar{\mathbf{C}}_f^T)/\epsilon)$ fulfilled by Assumption 1, where subscript “ff” denotes fastest subsystem. The complete input for the system (17), obtained from (37) and (41), has the form

$$\nu = -\mathbf{L}^T \mathbf{z} \quad (43)$$

where $\mathbf{z} = [\mathbf{z}_1^T \quad \mathbf{z}_2^T \quad \mathbf{z}_3^T]^T$ and $\mathbf{L}^T = \bar{\mathbf{L}}^T \mathbf{T}^{-1}$ in which $\bar{\mathbf{L}}^T = [\mathbf{L}_s^T - \mathbf{L}_f^T \mathbf{M}^T \quad \epsilon(\mathbf{L}_s^T - \mathbf{L}_f^T \mathbf{M}^T) \mathbf{P}^T + \mathbf{L}_f^T]$ and \mathbf{T} is given by (18). This is the composite feedback gain, \mathbf{L} derived from the subsystem feedback gains designed independently

in three different stages using well-conditioned matrices, so that the original system (17) is asymptotically stable, i.e., $\psi(\mathbf{A}^T - \mathbf{C}^T \mathbf{L}^T) < 0$. Uniqueness in this three-stage design and subsequent advantages are summarized as follows.

- 1) The lower triangular form (28) of (19) is attained by solving only two nonsymmetrical Riccati equations (23) and (26) for \mathbf{P} and \mathbf{P}_s , respectively, and the three-stage design is performed by solving two Sylvester equations (33) and (40), respectively, for \mathbf{M}_s and \mathbf{M} , i.e., only four equations are required to be solved compared to six in [20], which reduced online computation time.
- 2) The calculations are done with the two-time-scale representation instead of three-time-scale one due to which computational complexity and offline computation time are significantly reduced, without the loss of accuracy and the freedom to design individual observer gains for local subsystems, i.e., slow, fast, and fastest subsystems.

Step by step design of the full-order observer can be carried out as follows.

Step 1: Obtain the dual system (19) from (16) by transposing submatrices and applying transformation (18).

Step 2: Construct system (20) by regrouping states of (19) as \mathbf{q}_a and \mathbf{q}_b .

Step 3: Solve (23) to get \mathbf{P}^T and determine $\bar{\mathbf{A}}_s^T$, $\bar{\mathbf{A}}_f^T$, and $\bar{\mathbf{C}}_s^T$.

Step 4: Represent $\bar{\mathbf{A}}_s^T$ and $\bar{\mathbf{C}}_s^T$ in the partitioned form (24).

Step 5: Evaluate (26) for \mathbf{P}_s^T and find $\bar{\mathbf{A}}_{ss}^T$, $\bar{\mathbf{A}}_{sf}^T$, and $\bar{\mathbf{C}}_{ss}^T$.

Step 6: Determine \mathbf{L}_{ss}^T to position slow observer eigenvalues at preferred locations, i.e., $\psi(\bar{\mathbf{A}}_{ss}^T - \bar{\mathbf{C}}_{ss}^T \mathbf{L}_{ss}^T) = \psi_s^{\text{desired}}$.

Step 7: Calculate \mathbf{M}_s^T in (33) and obtain $\bar{\mathbf{C}}_{sf}^T$.

Step 8: Place eigenvalues of fast observer by determining \mathbf{L}_{sf}^T , such that $\psi((\bar{\mathbf{A}}_{sf}^T - \bar{\mathbf{C}}_{sf}^T \mathbf{L}_{sf}^T)/\mu) = \psi_f^{\text{desired}}$.

Step 9: Form \mathbf{L}_s^T as shown in (36), evaluate (40) for \mathbf{M}^T and find $\bar{\mathbf{C}}_f^T$.

Step 10: Assign fastest observer eigenvalues at desired locations by determining \mathbf{L}_f^T , so that $\psi((\bar{\mathbf{A}}_f^T - \bar{\mathbf{C}}_f^T \mathbf{L}_f^T)/\epsilon) = \psi_{ff}^{\text{desired}}$.

Step 11: Formulate composite observer gain \mathbf{L}^T as per (43) and check $\psi(\mathbf{A}^T - \mathbf{C}^T \mathbf{L}^T) = \psi_{ff}^{\text{desired}} \cup \psi_f^{\text{desired}} \cup \psi_s^{\text{desired}}$.

B. Reduced-Order Observer Design

1) Estimation of Slow and Fast States: In this case, it is assumed that \mathbf{x}_1 and \mathbf{x}_2 are to be estimated by an observer and \mathbf{x}_3 is to be determined from the outputs. Because of this, output $\mathbf{y} \in \mathbb{R}^{n_3}$ implying $\text{rank}(\mathbf{C}) = n_3$ as per Assumption 2. For the same, system (16) is redefined as

$$\left. \begin{aligned} \dot{\mathbf{x}}_{sf1} &= \mathbf{A}_{sf11} \mathbf{x}_{sf1} + \mathbf{A}_{sf12} \mathbf{x}_3 + \mathbf{B}_{sf1} \mathbf{u} \\ \epsilon \dot{\mathbf{x}}_3 &= \mathbf{A}_{sf21} \mathbf{x}_{sf1} + \mathbf{A}_{33} \mathbf{x}_3 + \mathbf{B}_3 \mathbf{u} \\ \mathbf{y} &= \mathbf{x}_3 \end{aligned} \right\} \quad (44)$$

where states to be estimated $\mathbf{x}_{sf1} = [\mathbf{x}_1^T \ \mathbf{x}_2^T]^T$ and

$$\mathbf{A}_{sf11} = \begin{bmatrix} \mathbf{A}_{11} & \mathbf{A}_{12} \\ \frac{\mathbf{A}_{21}}{\mu} & \frac{\mathbf{A}_{22}}{\mu} \end{bmatrix}, \quad \mathbf{A}_{sf12} = \begin{bmatrix} \mathbf{A}_{13} \\ \frac{\mathbf{A}_{23}}{\mu} \end{bmatrix}$$

$$\mathbf{A}_{sf21} = [\mathbf{A}_{31} \ \mathbf{A}_{32}], \quad \mathbf{B}_{sf1} = \begin{bmatrix} \mathbf{B}_1^T & \frac{\mathbf{B}_2^T}{\mu} \end{bmatrix}^T.$$

The reduced-order observer [25] for (44) has the form

$$\dot{\hat{\mathbf{x}}}_{sf} = \mathbf{A}_{sf} \hat{\mathbf{x}}_{sf} + \mathbf{B}_{sf} \mathbf{u} + \mathbf{L}_{sf} \mathbf{y} \quad (45)$$

where $\mathbf{A}_{sf} = \mathbf{A}_{sf11} - (1/\epsilon) \mathbf{L}_{sf1} \mathbf{A}_{sf21}$, $\mathbf{B}_{sf} = \mathbf{B}_{sf1} - (1/\epsilon) \mathbf{L}_{sf1} \mathbf{B}_3$, $\mathbf{L}_{sf} = \mathbf{A}_{sf} \mathbf{L}_{sf1} - (1/\epsilon) \mathbf{L}_{sf1} \mathbf{A}_{33} + \mathbf{A}_{sf12}$, and the state estimation is obtained as $\hat{\mathbf{x}}_{sf} = \hat{\mathbf{x}}_{sf1} - \mathbf{L}_{sf1} \mathbf{x}_3$. The observer gain matrix \mathbf{L}_{sf1} is determined, to stabilize (45), by the two-stage design procedure, analogous to two-stage feedback control design [26]. For designing an observer for (44), with \mathbf{x}_{sf1} immeasurable and \mathbf{x}_3 measurable states, following dual form is obtained:

$$\begin{bmatrix} \dot{\mathbf{z}}_1 \\ \dot{\mathbf{z}}_2 \end{bmatrix} = \begin{bmatrix} \mathbf{A}_{11}^T & \frac{\mathbf{A}_{21}^T}{\mu} \\ \mathbf{A}_{12}^T & \frac{\mathbf{A}_{22}^T}{\mu} \end{bmatrix} \begin{bmatrix} \mathbf{z}_1 \\ \mathbf{z}_2 \end{bmatrix} + \begin{bmatrix} \frac{\mathbf{A}_{31}^T}{\epsilon} \\ \frac{\mathbf{A}_{32}^T}{\mu} \end{bmatrix} \mathbf{v}. \quad (46)$$

Using $\mathbf{q}_1 = \epsilon \mathbf{z}_1$ and $\mathbf{q}_2 = (\epsilon/\mu) \mathbf{z}_2$, system (46) is changed to

$$\begin{bmatrix} \dot{\mathbf{q}}_1 \\ \dot{\mathbf{q}}_2 \end{bmatrix} = \begin{bmatrix} \mathbf{A}_{11}^T & \mathbf{A}_{21}^T \\ \frac{\mathbf{A}_{12}^T}{\mu} & \frac{\mathbf{A}_{22}^T}{\mu} \end{bmatrix} \begin{bmatrix} \mathbf{q}_1 \\ \mathbf{q}_2 \end{bmatrix} + \begin{bmatrix} \mathbf{A}_{31}^T \\ \frac{\mathbf{A}_{32}^T}{\mu} \end{bmatrix} \mathbf{v}. \quad (47)$$

Although (46) is having ϵ in it, the two-time-scale form (47) has a speed ratio of μ , which indeed represents that immeasurable states combine slow and fast dynamics and not the fastest one. Applying transformation $\mathbf{q}_s = \mathbf{q}_1 + \mu \mathbf{P}^T \mathbf{q}_2$ to (47) and following the procedure from (21) to (23) generates:

$$\begin{bmatrix} \dot{\mathbf{q}}_s \\ \dot{\mathbf{q}}_2 \end{bmatrix} = \begin{bmatrix} \mathbf{A}_s^T & \mathbf{0} \\ \frac{\mathbf{A}_{12}^T}{\mu} & \frac{\mathbf{A}_f^T}{\mu} \end{bmatrix} \begin{bmatrix} \mathbf{q}_s \\ \mathbf{q}_2 \end{bmatrix} + \begin{bmatrix} \mathbf{C}_s^T \\ \frac{\mathbf{A}_{32}^T}{\mu} \end{bmatrix} \mathbf{v} \quad (48)$$

where $\mathbf{A}_s^T = \mathbf{A}_{11}^T + \mathbf{P}^T \mathbf{A}_{12}^T$, $\mathbf{A}_f^T = \mathbf{A}_{22}^T - \mu \mathbf{A}_{12}^T \mathbf{P}^T$, and $\mathbf{C}_s^T = \mathbf{A}_{31}^T + \mathbf{P}^T \mathbf{A}_{32}^T$. In the first stage, applying $\mathbf{v} = -\mathbf{L}_s^T \mathbf{q}_s + \mathbf{v}_f$ to (48) gives

$$\begin{bmatrix} \dot{\mathbf{q}}_s \\ \dot{\mathbf{q}}_2 \end{bmatrix} = \begin{bmatrix} \mathbf{A}_s^T - \mathbf{C}_s^T \mathbf{L}_s^T & \mathbf{0} \\ \frac{\mathbf{A}_{12}^T - \mathbf{A}_{32}^T \mathbf{L}_s^T}{\mu} & \frac{\mathbf{A}_f^T}{\mu} \end{bmatrix} \begin{bmatrix} \mathbf{q}_s \\ \mathbf{q}_2 \end{bmatrix} + \begin{bmatrix} \mathbf{C}_s^T \\ \frac{\mathbf{A}_{32}^T}{\mu} \end{bmatrix} \mathbf{v}_f \quad (49)$$

where \mathbf{L}_s^T is selected such that $\psi(\mathbf{A}_s^T - \mathbf{C}_s^T \mathbf{L}_s^T) = \psi_s^{\text{desired}}$. Later, introducing $\mathbf{q}_f = -\mathbf{M}^T \mathbf{q}_s + \mathbf{q}_2$ for (49) and following steps from (38) to (40) yields:

$$\begin{bmatrix} \dot{\mathbf{q}}_s \\ \dot{\mathbf{q}}_f \end{bmatrix} = \begin{bmatrix} \mathbf{A}_s^T - \mathbf{C}_s^T \mathbf{L}_s^T & \mathbf{0} \\ \mathbf{0} & \frac{\mathbf{A}_f^T}{\mu} \end{bmatrix} \begin{bmatrix} \mathbf{q}_s \\ \mathbf{q}_f \end{bmatrix} + \begin{bmatrix} \mathbf{C}_s^T \\ \frac{\mathbf{C}_f^T}{\mu} \end{bmatrix} \mathbf{v}_f \quad (50)$$

with $\mathbf{C}_f^T = \mathbf{A}_{32}^T - \mu \mathbf{M}^T \mathbf{C}_s^T$. In the second stage, $\mathbf{v}_f = -\mathbf{L}_f^T \mathbf{q}_f$ is given to the system (50) as

$$\begin{bmatrix} \dot{\mathbf{q}}_s \\ \dot{\mathbf{q}}_f \end{bmatrix} = \begin{bmatrix} \mathbf{A}_s^T - \mathbf{C}_s^T \mathbf{L}_s^T & -\mathbf{C}_s^T \mathbf{L}_f^T \\ \mathbf{0} & \frac{\mathbf{A}_f^T - \mathbf{C}_f^T \mathbf{L}_f^T}{\mu} \end{bmatrix} \begin{bmatrix} \mathbf{q}_s \\ \mathbf{q}_f \end{bmatrix} \quad (51)$$

so as to assign $\psi((\mathbf{A}_f^T - \mathbf{C}_f^T \mathbf{L}_f^T)/\mu) = \psi_f^{\text{desired}}$. Therefore, the overall input for (46) can be rewritten in original states as

$$\mathbf{v} = -\mathbf{L}_{sf1}^T [\mathbf{z}_1^T \ \mathbf{z}_2^T]^T \quad (52)$$

where $\mathbf{L}_{sf1}^T = [\epsilon(\mathbf{L}_s^T - \mathbf{L}_f^T \mathbf{M}^T) \ \epsilon(\mathbf{L}_s^T - \mathbf{L}_f^T \mathbf{M}^T) \mathbf{P}^T + (\epsilon/\mu) \mathbf{L}_f^T]$ is the composite gain, calculated from subsystem gains

designed separately, so that original system (46) is stabilized. Estimation error dynamics for slow and fast states are

$$\dot{\mathbf{e}}_{sf} = \left(\mathbf{A}_{sf11} - \frac{1}{\epsilon} \mathbf{L}_{sf1} \mathbf{A}_{sf21} \right) \mathbf{e}_{sf} \quad (53)$$

where $\dot{\mathbf{e}}_{sf} = \dot{\mathbf{x}}_{sf1} - \dot{\hat{\mathbf{x}}}_{sf1}$ suggesting that the appropriate selection of the gain \mathbf{L}_{sf1} , such that $\psi(\mathbf{A}_{sf11} - (1/\epsilon)\mathbf{L}_{sf1}\mathbf{A}_{sf21}) < 0$, can cause the estimation error to decay to zero. Also, here, the pair $(\mathbf{A}_{sf11}, \mathbf{A}_{sf21})$ needs to be observable, which is satisfied by Assumption 1. Observability of $(\mathbf{A}_{sf11}, \mathbf{A}_{sf21})$ in the presence of observable pair (\mathbf{A}, \mathbf{C}) is proven in [27].

2) *Estimation of Some States in Both Slow and Fast Modes:* Consider that l_1 states of \mathbf{x}_1 and l_2 states of \mathbf{x}_2 are not available for measurement, defined as

$$\mathbf{x}_1 = [\mathbf{x}_{11}^T \ \mathbf{x}_{12}^T]^T \text{ and } \mathbf{x}_2 = [\mathbf{x}_{21}^T \ \mathbf{x}_{22}^T]^T \quad (54)$$

where $\mathbf{x}_{11} \in \mathbb{R}^{n_1-l_1}$, $\mathbf{x}_{12} \in \mathbb{R}^{l_1}$, $\mathbf{x}_{21} \in \mathbb{R}^{l_2}$, and $\mathbf{x}_{22} \in \mathbb{R}^{n_2-l_2}$. Remaining all other states, including \mathbf{x}_{11} , \mathbf{x}_{22} , and \mathbf{x}_3 are measurable. As a consequence, the matrices \mathbf{A}_{ij} and \mathbf{B}_i in (16) are partitioned appropriately as

$$\begin{aligned} \mathbf{A}_{11} &= \begin{bmatrix} \mathbf{a}_{11} & \mathbf{a}_{12} \\ \mathbf{a}_{21} & \mathbf{a}_{22} \end{bmatrix}, \quad \mathbf{A}_{12} = \begin{bmatrix} \mathbf{a}_{13} & \mathbf{a}_{14} \\ \mathbf{a}_{23} & \mathbf{a}_{24} \end{bmatrix}, \quad \mathbf{A}_{13} = \begin{bmatrix} \mathbf{a}_{15} \\ \mathbf{a}_{25} \end{bmatrix} \\ \mathbf{A}_{21} &= \begin{bmatrix} \mathbf{a}_{31} & \mathbf{a}_{32} \\ \mathbf{a}_{41} & \mathbf{a}_{42} \end{bmatrix}, \quad \mathbf{A}_{22} = \begin{bmatrix} \mathbf{a}_{33} & \mathbf{a}_{34} \\ \mathbf{a}_{43} & \mathbf{a}_{44} \end{bmatrix}, \quad \mathbf{A}_{23} = \begin{bmatrix} \mathbf{a}_{35} \\ \mathbf{a}_{45} \end{bmatrix}, \\ \mathbf{A}_{31} &= [\mathbf{a}_{51} \ \mathbf{a}_{52}], \quad \mathbf{A}_{32} = [\mathbf{a}_{53} \ \mathbf{a}_{54}], \quad \mathbf{A}_3 = \mathbf{a}_{55} \\ \mathbf{B}_1 &= [\mathbf{b}_1^T \ \mathbf{b}_2^T]^T, \quad \mathbf{B}_2 = [\mathbf{b}_3^T \ \mathbf{b}_4^T]^T, \quad \mathbf{B}_3 = \mathbf{b}_5 \end{aligned}$$

where \mathbf{a}_{ij} and \mathbf{b}_i are of suitable dimensions. Regrouping of states as immeasurable and measurable, one can have

$$\left. \begin{aligned} \dot{\mathbf{x}}_{fs1} &= \mathbf{A}_{fs11}\mathbf{x}_{fs1} + \mathbf{A}_{fs12}\mathbf{x}_{fs2} + \mathbf{B}_{fs1}\mathbf{u} \\ \dot{\mathbf{x}}_{fs2} &= \mathbf{A}_{fs21}\mathbf{x}_{fs1} + \mathbf{A}_{fs22}\mathbf{x}_{fs2} + \mathbf{B}_{fs2}\mathbf{u} \\ \mathbf{y} &= \mathbf{x}_{fs2} \end{aligned} \right\} \quad (55)$$

where $\mathbf{x}_{fs1} = [\mathbf{x}_{12}^T \ \mathbf{x}_{21}^T]^T$, $\mathbf{x}_{fs2} = [\mathbf{x}_{11}^T \ \mathbf{x}_{22}^T \ \mathbf{x}_3^T]^T$, and

$$\begin{aligned} \mathbf{A}_{fs11} &= \begin{bmatrix} \mathbf{a}_{22} & \mathbf{a}_{23} \\ \mathbf{a}_{32} & \mathbf{a}_{33} \\ \mu & \mu \end{bmatrix}, \quad \mathbf{A}_{fs12} = \begin{bmatrix} \mathbf{a}_{21} & \mathbf{a}_{24} & \mathbf{a}_{25} \\ \mathbf{a}_{31} & \mathbf{a}_{34} & \mathbf{a}_{35} \\ \mu & \mu & \mu \end{bmatrix} \\ \mathbf{A}_{fs21} &= \begin{bmatrix} \mathbf{a}_{12} & \mathbf{a}_{13} \\ \mathbf{a}_{42} & \mathbf{a}_{43} \\ \mu & \mu \\ \mathbf{a}_{52} & \mathbf{a}_{53} \\ \epsilon & \epsilon \end{bmatrix}, \quad \mathbf{A}_{fs22} = \begin{bmatrix} \mathbf{a}_{11} & \mathbf{a}_{14} & \mathbf{a}_{15} \\ \mathbf{a}_{41} & \mathbf{a}_{44} & \mathbf{a}_{45} \\ \mu & \mu & \mu \\ \mathbf{a}_{51} & \mathbf{a}_{53} & \mathbf{a}_{55} \\ \epsilon & \epsilon & \epsilon \end{bmatrix} \\ \mathbf{B}_{fs1} &= \begin{bmatrix} \mathbf{b}_2^T \\ \mathbf{b}_3^T \\ \mu \end{bmatrix}^T, \quad \mathbf{B}_{fs2} = \begin{bmatrix} \mathbf{b}_1^T & \mathbf{b}_4^T & \mathbf{b}_5^T \\ \mu & \epsilon & \epsilon \end{bmatrix}^T. \end{aligned}$$

The corresponding reduced-order observer [25] for (55) is

$$\dot{\hat{\mathbf{x}}}_{fs} = \mathbf{A}_{fs}\hat{\mathbf{x}}_{fs} + \mathbf{B}_{fs}\mathbf{u} + \mathbf{L}_{fs}\mathbf{y} \quad (56)$$

where $\mathbf{A}_{fs} = \mathbf{A}_{fs11} - \mathbf{L}_{fs1}\mathbf{A}_{fs21}$, $\mathbf{B}_{fs} = \mathbf{B}_{fs1} - \mathbf{L}_{fs1}\mathbf{B}_{fs2}$, and $\mathbf{L}_{fs} = \mathbf{A}_{fs}\mathbf{L}_{fs1} - \mathbf{L}_{fs1}\mathbf{A}_{fs22} + \mathbf{A}_{fs12}$ with state estimation as $\hat{\mathbf{x}}_{fs} = \hat{\mathbf{x}}_{fs1} - \mathbf{L}_{fs1}\mathbf{x}_{fs2}$, where \mathbf{L}_{fs1} is the reduced-order composite observer gain of order $((l_1 + l_2) \times (n_3 + (n_1 - l_1) + (n_2 - l_2)))$. This can also be derived by the two-stage design (refer Section III-B1). The aim of the observer (56) is to construct immeasurable states \mathbf{x}_{fs1} in an asymptotic manner in the sense that $\dot{\mathbf{e}}_{fs} = (\mathbf{A}_{fs11} - \mathbf{L}_{fs1}\mathbf{A}_{fs21})\mathbf{e}_{fs}$ tends to zero. To achieve this goal \mathbf{L}_{fs1} is chosen such that the matrix

$(\mathbf{A}_{fs11} - \mathbf{L}_{fs1}\mathbf{A}_{fs21})$ is asymptotically stable. It is possible if the pair $(\mathbf{A}_{fs11}, \mathbf{A}_{fs21})$ is observable.

Comment 1: For the reduced-order observer with any combination of inaccessible states, an appropriate regrouping of states, similar to (55), can simplify the observer design procedure. If the inaccessible states include few states from slow, fast, and fastest modes then the three-stage design and if they include states from any two modes then the two-stage design is recommended.

Novelty in the reduced-order observer design and resulting benefits are briefed as follows.

- 1) The triangular form (48) of (47) is reached by solving a nonsymmetrical Riccati equation (23) for \mathbf{P} and then the two-stage design is done by solving a Sylvester equation (40) for \mathbf{M} , i.e., only two algebraic equations are required to be evaluated compared to three equations in [15], thereby reducing computation time.
- 2) As only two transformations are used, one for getting the lower triangular form (48) and the other for block diagonal form (50), the computational complexity and offline computation time are lowered considerably.
- 3) Independently designed observer gains (in both two-stage and three-stage) result in the improvement of robustness and reliability of the system.

The reduced-order observer by the three-stage design can be completed as per the steps given at the end of Section III-A. Steps for the two-stage design are enumerated as follows.

Step 1: Obtain the dual system (47) by transposing submatrices associated with the immeasurable states (in this case, \mathbf{x}_{sf1}).

Step 2: Get the value of \mathbf{P}^T by solving equation similar to (23) and determine \mathbf{A}_s^T , \mathbf{A}_f^T , and \mathbf{C}_s^T .

Step 3: Compute \mathbf{L}_s^T to position slow subsystem observer eigenvalues at selected locations, i.e., $\psi(\mathbf{A}_s^T - \mathbf{C}_s^T\mathbf{L}_s^T) = \psi_s^{\text{desired}}$.

Step 4: Evaluate equation similar to (40) for \mathbf{M}^T and estimate $\tilde{\mathbf{C}}_f^T$.

Step 5: Allocate fast observer eigenvalues at chosen locations by determining \mathbf{L}_f^T , namely, $\psi((\mathbf{A}_f^T - \mathbf{C}_f^T\mathbf{L}_f^T)/\mu) = \psi_f^{\text{desired}}$.

Step 6: Formulate composite observer gain \mathbf{L}_{sf1}^T as per (52) and test $\psi(\mathbf{A}_{sf11}^T - \mathbf{A}_{sf12}^T\mathbf{L}_{sf1}^T) = \psi_f^{\text{desired}} \cup \psi_s^{\text{desired}}$.

IV. DESIGN AND APPLICATION OF OBSERVERS TO AHWR

This section corroborates the proposal of the observers, designed in Section III, for the nonlinear system of AHWR. The AHWR model (15) is structured into a three-time-scale form (16) first and then observers are formulated for it.

A. Three-Time-Scale Representation of AHWR Model

Partitioning of a multitime-scale system into several subsystems can be done on the basis of physical nature of the system, mathematical conditions, specific control requirements, grouping of state variables, and so on [12]. In case of AHWR, three distinct clusters of eigenvalues help to identify the three-time-scale nature, i.e., 90 eigenvalues are grouped into 38 slow, 35 fast, and 17 fastest eigenvalues. Thus, μ and ϵ

are calculated as ratios of magnitudes of eigenvalues from respective clusters

$$\mu = \frac{\max|\psi_s|}{\min|\psi_f|} = 5.3399 \times 10^{-1}$$

$$\epsilon = \frac{\max|\psi_s|}{\min|\psi_{ff}|} = 8.6741 \times 10^{-4}.$$

For obtaining an explicit singular perturbation form of AHWR, i.e., a model with first, second, and third subsystems with, respectively, slow, fast, and fastest eigenvalues and nonsingular matrices \mathbf{A}_{22} and \mathbf{A}_{33} (i.e., satisfying Assumption 3), state vector of the system (15) is partitioned as

$$\begin{cases} \mathbf{x}_1 = [\mathbf{x}_H^T & \mathbf{x}_X^T & \mathbf{x}_I^T]^T \\ \mathbf{x}_2 = [\delta h_d & \mathbf{x}_C^T & \mathbf{x}_x^T]^T \\ \mathbf{x}_3 = \mathbf{x}_P \end{cases}. \quad (57)$$

Accordingly, “slow” states include RR positions, xenon, and iodine concentrations, “fast” states contain downcomer enthalpy, precursors’ concentrations, and exit quality, and “fastest” states comprise nodal powers. Recall that the system (15) also fulfills Assumption 1. Feed-flow rate, q_f is a function of total power and \mathbf{B}_f is a column vector of dimension 90 with a single entry at 39th position. Hence, the input δq_f is treated separately and is not considered in the three-time-scale form of AHWR. Now, as per (57), submatrices \mathbf{A}_{ij} , \mathbf{B}_i , and \mathbf{C}_i are obtained from (15) and a singularly perturbed three-time-scale structure (16) is obtained.

B. Observer Designs

A full-order observer is designed as per the procedure expressed in Section III-A. In this, the normalized nodal powers of the nonlinear AHWR system are compared with the observer outputs and the generated error is given to a composite observer gain. Other inputs to an observer are controller output \mathbf{u}_s and δq_f . The estimated states are then fed to a state feedback controller, designed in [21], to generate \mathbf{u}_s .

Afterward, a reduced-order observer is designed to estimate xenon, iodine, and precursors’ concentrations using the technique in Section III-B2. The state vector (8) is divided, respectively, into immeasurable and measurable states as

$$\begin{cases} \mathbf{x}_{fs1} = [\mathbf{x}_X^T & \mathbf{x}_I^T & \mathbf{x}_C^T]^T \\ \mathbf{x}_{fs2} = [\mathbf{x}_H^T & \delta h_d & \mathbf{x}_x^T & \mathbf{x}_P^T]^T \end{cases}. \quad (58)$$

Immeasurable states include 34 slow and 17 fast states, making an order of observer as 51. Here, normalized measurable states along with \mathbf{u}_s and δq_f are inputs to a reduced-order observer for state estimation. The estimated states and measurable states are then passed to the same controller [21] to generate the control signal.

Considering both the fast convergence rate for estimation error and sufficient degree of noise smoothing, observer closed-loop eigenvalues are selected six times faster than the system closed-loop eigenvalues [27]. This also facilitates to maintain an appropriate speed ratio between slow, fast, and fastest observer eigenvalues and satisfy Assumptions 4 and 5 for both three-stage and two-stage designs. For a rational comparison of observers, out of the 90 eigenvalues of the full-order

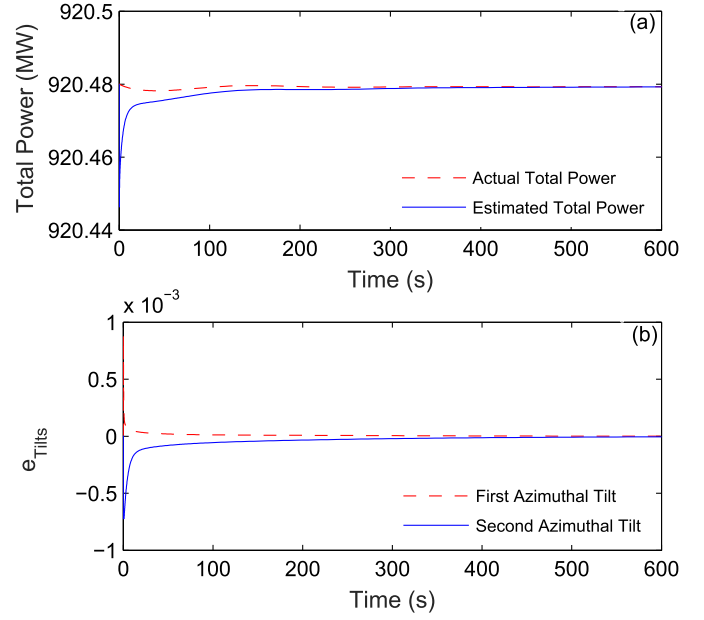


Fig. 1. Results for mismatch in initial conditions with a full-order observer. (a) Total reactor power. (b) Estimation errors for azimuthal tilts.

observer, 51 eigenvalues for the reduced-order observer are chosen very carefully so that the eigenvalues for xenon, iodine, and precursors’ concentrations are the same, in both the observer designs.

V. TRANSIENT SIMULATIONS

Here, it is shown that the AHWR, represented by (1)–(7), achieves spatial stabilization with a state feedback controller [21], fed by the states computed using proposed observers.

Initially, the closed-loop response of the system to the difference in initial conditions of estimated and actual states is studied to highlight the effectiveness of suggested observers. In this, the initial conditions of all the estimated states are perturbed by 0.01%. Fig. 1(a) compares estimated total reactor power due to full-order observer with actual power. It is observed that the estimated total power attains a steady-state value of 920.48 MW in approximately 300 s. Nodal power estimations are displayed in Fig. 1(b) as variations in the estimation errors, calculated for azimuthal tilts [22]. These errors also decay in about 300 s. Estimation errors for xenon, iodine, and precursor concentrations in node 1 by both full- and reduced-order observers are also plotted in Fig. 2. The estimation errors for xenon and iodine concentrations reach zero in about 300 s [Fig. 2(a) and (b)] while it takes just 110 s for precursor concentration [Fig. 2(c)]. Even if the estimation errors for xenon and iodine take more time to decay they are very small. As the similar kind of result is viewed for all the nodal variables, the initial mismatches are efficaciously taken care by the advised method.

In other transients mentioned below, results of advocated observer-based controls are compared with controller [21] (without an observer) and fast output sampling technique [28].

Herein, the reactor is ensured to be operating at the steady state and suddenly RR4 is moved out manually by 1% after

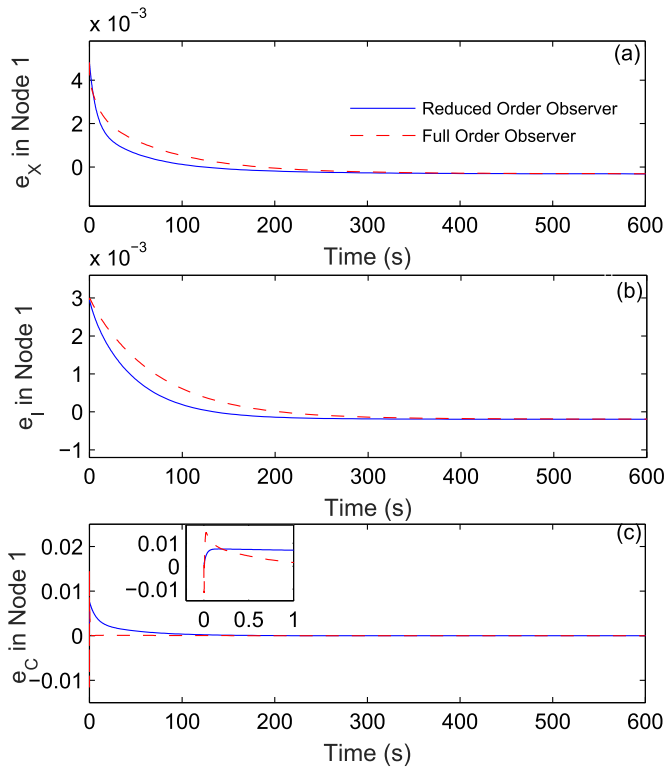


Fig. 2. Estimation errors for (a) xenon, (b) iodine, (c) precursors concentrations in node 1 for mismatch in initial conditions.

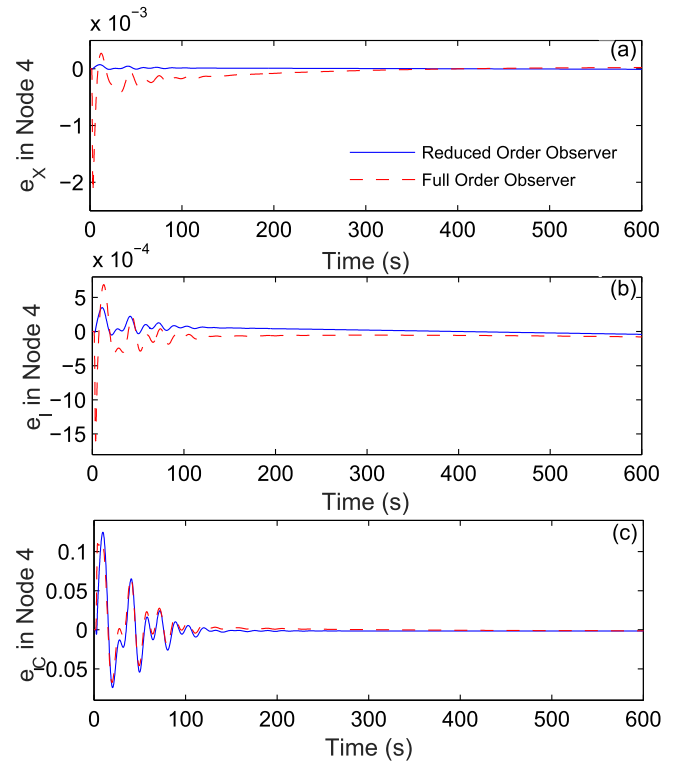


Fig. 4. Estimation errors for (a) xenon, (b) iodine, and (c) precursor concentrations in node 4 due to the transient generated by RR4.

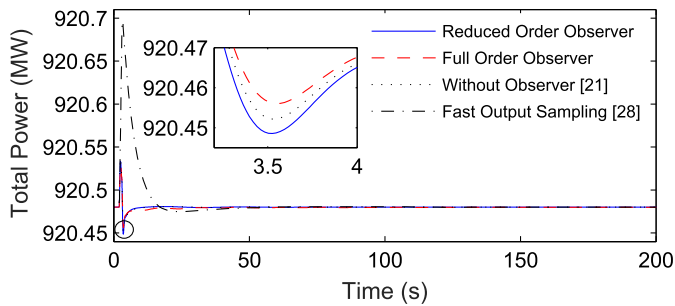


Fig. 3. Results for total reactor power due to the transient generated by RR4.

2 s and thereafter it is restored. Variations in the total power, as a result of this transient, for all the controls are indicated in Fig. 3. The zoomed-in view of Fig. 3 (marked by a small circle) signifies that the observers estimate the total power with reasonably good accuracy. Estimation errors determined for xenon, iodine, and precursor concentrations in node 4 due to full- and reduced-order observers are presented in Fig. 4. Observing Fig. 4, it can be noticed that the estimation errors with a reduced-order observer are converging faster than the full-order observer.

Fig. 5 compares the total power variations for the transient involving power maneuvering. In this case, the demand power is decreased from 920.48 to 828.43 MW at the rate of 1.5 MW/s, in approximately 61 s and is held constant thereafter. From Fig. 5, it is evident that during power maneuvering, the total power due to reduced-order observer is maintained close to the power obtained with [21]. Once the steady state

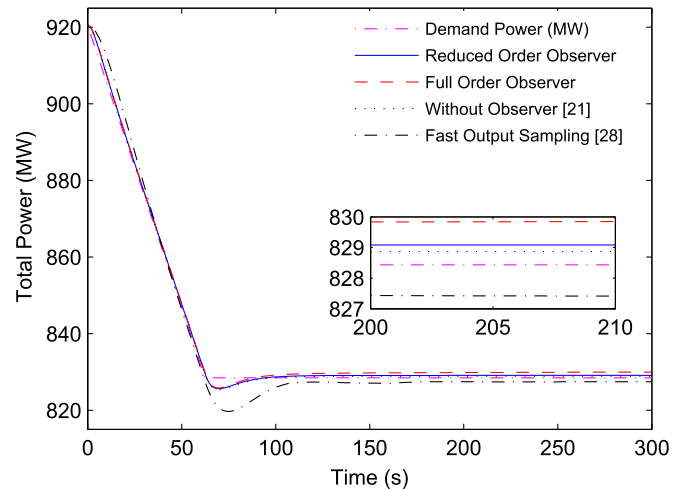


Fig. 5. Total power variations during power maneuvering from 920.48 to 828.43 MW.

is gained, it does not show any variation during the remaining prolonged simulation.

Finally, in order to evaluate the response of the system to a disturbance, a nonlinear model was simulated with a +5% step change in feed flow after 60 s. As a consequence, the total power shows variations as depicted in Fig. 6. In order to maintain the total power at an equilibrium level, all the RRs are moved inside almost by 1%. All the RRs (RR2, RR4, RR6, and RR8) under the influence of a particular controller exhibited similar variations [Fig. 7(a)] except for full-order observer [Fig. 7(b)]. With a full-order observer scheme, RR2 and

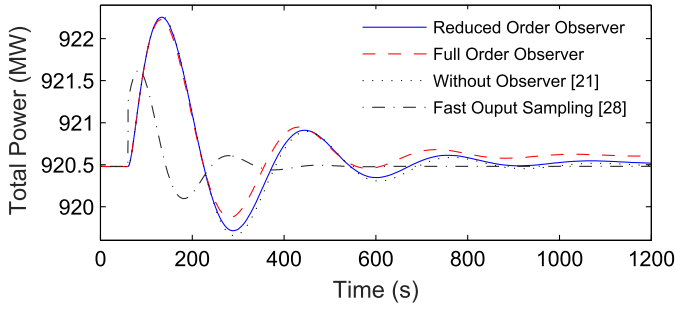


Fig. 6. Variations in total reactor power due to step change in the feed flow.

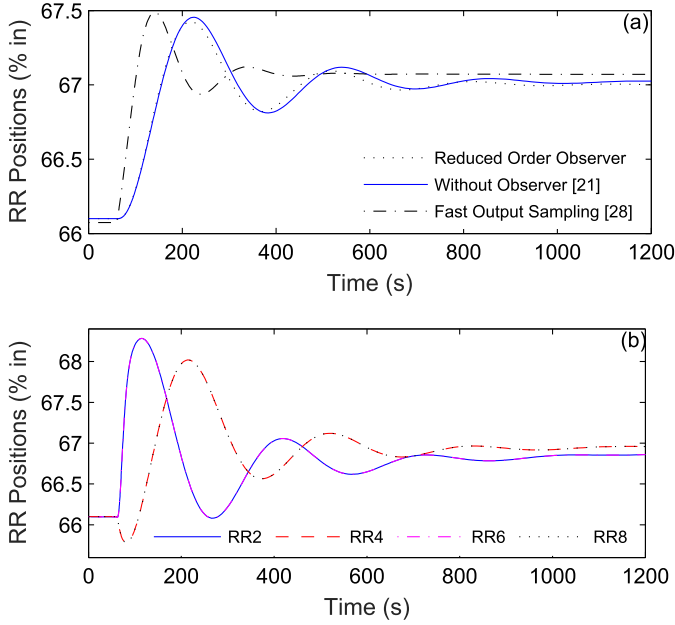


Fig. 7. Variations in RR positions due to a step change in the feed flow (a) with reduced-order observer, without an observer, and fast output sampling and (b) full-order observer.

RR6 reported the same deviations and RR6 and RR8 displayed the identical movements as illustrated in Fig. 7(b). Although the performance of the fast output sampling technique is found to be better, for regulation and tracking its performance is not acceptable over reduced-order observer-based control. The performance with reduced-order observer is superior to full-order observer in this transient too.

In summary, the nonlinear AHWR system achieves spatial stabilization with the observers integrated with the controller [21] under various transients. Comparison with [21] shows that the observers combined with the same controller provide almost identical performance under all the transients, thus circumventing the need for expensive sensors to measure all the variables. When compared with the fast output sampling technique, submitted designs demonstrate performance dominance due to the availability of all the states (either estimated or both estimated and measured) for feedback in contrast to only the outputs in the fast output sampling. Among the full- and reduced-order observers, the improved performance is attained with the reduced-order observer due to two reasons. First, the full-order observer has to estimate

all the 90 states with the help of outputs, i.e., 17 nodal powers. On the other hand, the reduced-order observer has to estimate 51 states with the help of 39 states which include RR positions in 4 nodes, an enthalpy, exit quality, and nodal powers in 17 nodes, i.e., the number of inputs for the reduced-order observer is more compared to the full-order observer. Second, in the reduced-order observer, RR positions are assumed to be available for the measurement, which are the function of inputs, i.e., voltage signals to RR positions. Finally, the convergence of the observer depends on the eigenvalues. This convergence can further be improved and finer results can be obtained by the optimization. These simulations serve to simply establish the applicability of the suggested simple linear observers to a nonlinear plant.

VI. CONCLUSION

In this paper, full- and reduced-order observers are formulated for AHWR to estimate xenon, iodine, and precursors' concentrations. These observers are combined with a feedback controller and nonlinear system behavior is assessed under representative transients. Presented observer designs are based on the separation of slow, fast, and fastest states, hence, the problem of handling higher order ill-conditioned matrices of singularly perturbed three-time-scale is alleviated. First, a full-order observer is designed in independent three stages and then the reduced-order observer is designed in two stages. Two-stage observer design is done by solving only two algebraic equations, whereas the three-stage design is completed creatively by applying the two-stage design twice, i.e., by solving merely four algebraic equations. The suggested multistage designs reduce online and offline computational requirements significantly and also improve robustness and reliability of the closed-loop system. The nonlinear simulation results confirmed that the observers obtained by the time-scale decomposition can successfully stabilize an AHWR system. The presented observers have a great potential to implement modern state variable feedback control for the multitime-scale system.

ACKNOWLEDGMENT

The authors would like to thank the anonymous reviewers for constructive comments and suggestions to improve the quality of this paper.

REFERENCES

- [1] *Energy, Electricity and Nuclear Power Estimates for the Period Up to 2050*, Int. Atomic Energy Agency, Vienna, Austria, Sep. 2017.
- [2] G. Li, X. Wang, B. Liang, X. Li, B. Zhang, and Y. Zou, "Modeling and control of nuclear reactor cores for electricity generation: A review of advanced technologies," *Renew. Sustain. Energy Rev.*, vol. 60, pp. 116–128, Jul. 2016.
- [3] Y. H. Park and N. Z. Cho, "Estimation of neutron flux and xenon distributions via observer-based control theory," *Nucl. Sci. Eng.*, vol. 111, no. 1, pp. 66–81, 1992.
- [4] P. Wang, T. Aldemir, and V. I. Utkin, "Estimation of xenon concentration and reactivity in nuclear reactors using sliding mode observers," in *Proc. IEEE Conf. Decis. Control*, vol. 2, Dec. 2001, pp. 1801–1806.
- [5] M. H. Esteki, G. R. Ansarifard, and M. Arghand, "Estimation of the xenon concentration and delayed neutrons precursors densities in the pressurized-water nuclear reactors (PWR) with sliding mode observer considering xenon oscillations," *Ann. Nucl. Energy*, vol. 77, pp. 1–22, Mar. 2015.

- [6] S. Hussain, A. I. Bhatti, A. Samee, and S. H. Kaiser, "Estimation of precursor density of a power reactor using uniform second order sliding mode observer," *Ann. Nucl. Energy*, vol. 54, pp. 233–239, Apr. 2013.
- [7] S. Hussain, A. I. Bhatti, A. Samee, and S. H. Kaiser, "Estimation of reactivity and average fuel temperature of a pressurized water reactor using sliding mode differentiator observer," *IEEE Trans. Nucl. Sci.*, vol. 60, no. 4, pp. 3025–3032, Aug. 2013.
- [8] M. H. Z. Yeganeh and G. R. Ansarifar, "Estimation of the poisons reactivity in the P.W.R Nuclear Reactors using modified higher order sliding mode observer based on the multi-point nuclear reactor model," *Ann. Nucl. Energy*, vol. 112, pp. 158–169, Feb. 2018.
- [9] Z. Dong, X. Huang, D. Li, and Z. Zhang, "Reactivity estimation based on an extended state observer of neutron kinetics," *IEEE Trans. Nucl. Sci.*, vol. 63, no. 5, pp. 2691–2697, Oct. 2016.
- [10] S. B. Patel, S. Mukhopadhyay, and A. P. Tiwari, "Estimation of reactivity and delayed neutron precursorsâTM concentrations using a multiscale extended Kalman filter," *Ann. Nucl. Energy*, vol. 111, pp. 666–675, Jan. 2018.
- [11] A. P. Tiwari and B. Bandyopadhyay, "Control of xenon induced spatial oscillations in a large PHWR," in *Proc. IEEE Int. Conf. Global Connectivity Energy, Comput., Commun. Control*, vol. 1, Dec. 1998, pp. 178–181.
- [12] Y. Zhang, D. S. Naidu, C. Cai, and A. Y. Zou, "Singular perturbations and time scales in control theories and applications: An overview 2002–2012," *Int. J. Inf. Syst. Sci.*, vol. 9, no. 1, pp. 1–36, 2014.
- [13] J. O'Reilly, "Dynamical feedback control for a class of singularly perturbed linear systems using a full-order observer," *Int. J. Control*, vol. 31, no. 1, pp. 1–10, 1980.
- [14] K. R. Shouse and D. G. Taylor, "Reduced-order discrete-time recursive observers for linear continuous-time singularly perturbed systems," in *Proc. Amer. Control Conf.*, Jun. 1993, pp. 2128–2129.
- [15] H. Yoo and Z. Gajic, "New designs of linear observers and observer-based controllers for singularly perturbed linear systems," *IEEE Trans. Autom. Control*, to be published, doi: [10.1109/TAC.2018.2814920](https://doi.org/10.1109/TAC.2018.2814920).
- [16] H. Yoo and Z. Gajic, "New designs of reduced-order observer-based controllers for singularly perturbed linear systems," *Math. Problems Eng.*, vol. 2017, pp. 1–14, Dec. 2017.
- [17] C.-C. Tsui, "Observer design—A survey," *Int. J. Autom. Comput.*, vol. 12, no. 1, pp. 50–61, 2015.
- [18] C. Yang, L. Zhang, and L. Zhou, "Observer design for singularly perturbed systems with multirate sampled and delayed measurements," *J. Dyn. Syst., Meas. Control*, vol. 138, no. 5, pp. 051007-1–051007-9, 2016.
- [19] R. K. Munje, B. M. Patre, P. S. Londhe, A. P. Tiwari, and S. R. Shimjith, "Investigation of spatial control strategies for AHWR: A comparative study," *IEEE Trans. Nucl. Sci.*, vol. 63, no. 2, pp. 1236–1246, Apr. 2016.
- [20] V. Radisavljevic-Gajic, M. Milanovic, and G. Clayton, "Three-stage feedback controller design with applications to three time-scale linear control systems," *ASME J. Dyn. Syst., Meas., Control*, vol. 139, pp. 104502-1–104502-10, Oct. 2017.
- [21] R. K. Munje, J. G. Parkhe, and B. M. Patre, "Control of xenon oscillations in advanced heavy water reactor via two-stage decomposition," *Ann. Nucl. Energy*, vol. 77, pp. 326–334, Mar. 2015.
- [22] S. R. Shimjith, A. P. Tiwari, B. Bandyopadhyay, and R. K. Patil, "Spatial stabilization of advanced heavy water reactor," *Ann. Nucl. Energy*, vol. 38, pp. 1545–1558, Jul. 2011.
- [23] R. K. Sinha and A. Kakodkar, "Design and development of the AHWR—The Indian thorium fuelled innovative nuclear reactor," *Nucl. Eng. Des.*, vol. 236, pp. 683–700, Apr. 2006.
- [24] D. S. Naidu, *Singular Perturbation Methodology in Control Systems*. London, U.K.: Peregrinus, 1988.
- [25] C.-T. Chen, *Linear System Theory and Design*. New York, NY, USA: Oxford Univ. Press, 1999.
- [26] V. Radisavljevic-Gajic and P. Rose, "A new two-stage design of feedback controllers for a hydrogen gas reformer," *Int. J. Hydrogen Energy*, vol. 39, no. 22, pp. 11738–11748, 2014.
- [27] V. Radisavljevic-Gajic, "Full- and reduced-order linear observer implementations in MATLAB/Simulink [Lecture Notes]," *IEEE Control Syst. Mag.*, vol. 35, no. 5, pp. 91–101, Oct. 2015.
- [28] R. K. Munje, P. S. Londhe, J. G. Parkhe, B. M. Patre, and A. P. Tiwari, "Spatial control of advanced heavy water reactor by fast output sampling technique," in *Proc. IEEE Int. Conf. Control Appl.*, Aug. 2013, pp. 1212–1217.